

Temporal Homogenization of Viscoelastic and Viscoplastic Solids Subjected to Locally Periodic Loading

Qing Yu and Jacob Fish

*Departments of Civil Engineering, Mechanical and Aeronautical Engineering
Rensselaer Polytechnic Institute, Troy, NY 12180*

Abstract: As a direct extension of the asymptotic spatial homogenization method we develop a temporal homogenization scheme for a class of homogeneous solids with an intrinsic time scale significantly longer than a period of prescribed loading. Two rate-dependent material models, the Maxwell viscoelastic model and the power-law viscoplastic model, are studied as an illustrative examples. Double scale asymptotic analysis in time domain is utilized to obtain a sequence of initial-boundary value problems with various orders of temporal scaling parameter. It is shown that various order initial-boundary value problems can be further decomposed into: (i) the global initial-boundary value problem with smooth loading for the entire loading history, and (ii) the local initial-boundary value problem with the remaining (oscillatory) portion of loading for a single load period. Large time increments can be used for integrating the global problem due to smooth loading, whereas the integration of the local initial-boundary value problem requires a significantly smaller time step, but only locally in a single load period. The present temporal homogenization approach has been found to be in good agreement with a closed-form analytical solution for one-dimensional case and with a numerical solution in multidimensional case obtained by using a sufficiently small time step required to resolve the load oscillations.

1.0 Introduction

Mathematical homogenization method has been widely used for solving initial-boundary value problems with oscillatory coefficients. The validity of the asymptotic homogenization depends on the existence of distinct multiple length scales in the physical processes so that a small positive scaling parameter quantifying the ratio between the scales can be identified. In general, multiple length scales may exist in both space and time domains, although most of the recent research efforts have been focussing on the spatial homogenization (see, for instance, [12][14]). In contrast to the spatial scale separation, which is typically induced by spatial heterogeneities, the multiple temporal scales can be attributed to at least three sources (or their combinations):

- *the interaction of multiple physical processes*

Different physical processes, such as mechanical, thermal, diffusion, and chemical reaction, may evolve along different time frames. Interaction between multiple physical processes requires consideration of relevant time frames within a single reference time coordinate. An example problem fall-

ing into this category is a coupled thermo-mechanical process, which has been studied by Boutin and Wong [2] using spatial-temporal homogenization approach. Most recently, a general setting for the spatial-temporal asymptotic homogenization theory has been established by Yu and Fish [15].

- *existence of spatial heterogeneities*

Spatial heterogeneities may cause dispersion of high frequency waves traveling in heterogeneous media. The time frame corresponding to the successive reflection and refraction of waves between the interfaces in microstructure could be significantly different from the time frame of the macroscopic wave motion. The earliest work on the multiple temporal scales induced by spatial heterogeneities is often attributed to Benssousan et al. [1] who studied parabolic equations with oscillatory coefficients. Francfort [8] utilized multiple temporal scales to analyze thermo-elastic composites. Kevorkin and Bosley [9] introduced an additional fast time scale to study the hyperbolic conservation laws with rapid spatial fluctuations. In the recent work Fish, Chen and Nagai [4][5] introduced multiple slow temporal scales to alleviate the problem of secularity caused by high order terms in the asymptotic analysis of wave propagation in heterogeneous solids and established a nonlocal continuum approach to capture dispersion effects [6][7].

- *existence multiple time scale within a single physical process on a single spatial scale*

In many engineering problems multiple temporal scales arise in a single physical process taking place in a homogeneous medium. For example, slow degradation of materials properties due to creep, relaxation and fatigue, subjected to rapidly oscillatory loading exhibit multiple temporal scales. This category of problems possess an intrinsic *slow* time scale, which may significantly differ from the frequency of external input.

In the present manuscript, we focus on the third category of problems. Attention is restricted to the asymptotic homogenization of rate-dependent solids. The prediction of long-term behavior of rate-dependent solids subjected to oscillatory loading requires significant computational resources, in particular, for nonlinear solids subjected to non-harmonic loading. This is because the resolution of high frequency loading requires time integration increments, which are much smaller than the observation time window. The primary objective of this manuscript is to develop a temporal homogenization scheme by which the initial-boundary value problem with locally periodic loading in time domain can be approximated by: (i) the global initial-boundary value problem with smooth loading for the entire loading history, and (ii) the local initial-boundary value problem with the remaining (oscillatory) portion of loading for a single load period in selected region(s) of the time domain.

For the global initial-boundary value problem a large time increment can be used, whereas the integration of the local initial-boundary value problem requires a significantly smaller time step, but only locally in the time domain, where a full response is sought. It is apparent that the present temporal homogenization approach closely resembles the classical spatial homogenization scheme. The global

initial value problem is equivalent to the macroscopic boundary value problem with homogenized coefficients, whereas the postprocessing of local fields within the Representative Volume Element (RVE) is equivalent to the local initial-boundary value problem in the temporal homogenization scheme. The main conceptual difference between the two will be shown to exist for nonlinear problems. For nonlinear heterogeneous solids both the macroscopic and the RVE problems are nonlinear, whereas the temporal homogenization of viscoplastic solids gives rise to nonlinear global initial-boundary value problem and a linear local initial-boundary value problem. It will be shown that nonlinearities do reappear in the higher order initial-boundary value problems, which can be used to improve the quality of the global-local approximation, but are rarely used in practice.

Two rate-dependent material models, the Maxwell viscoelastic model and the power-law viscoplastic model [10][11], are considered as illustrative examples. We start with the definition of multiple temporal scales in Section 2.1. In Section 2.2, the temporal homogenization scheme for the linear Maxwell viscoelastic model is presented. It is shown that a long-term response can be obtained by solving the time-averaged zero-order homogenized initial-boundary value problem along with the smooth portion of external loading. The deviation from the smooth solution is obtained by solving a local linear initial-boundary value problems within one period of load cycle. In Section 2.3, we extend the temporal homogenization scheme to the power-law viscoplastic solid. In Section 3 the temporal homogenization approach is verified against the closed-form reference solution for one-dimensional viscoelastic and viscoplastic solids. In multidimensions, two numerical examples comparing the temporal homogenized approach with the reference solutions obtained with a time step sufficiently small to resolve the local load fluctuations are described in Section 4.

2.0 Temporal homogenization of the rate-dependent solids subjected to locally periodic loading

2.1 Definition of multiple temporal scales

In the present work, we assume that the intrinsic time scale t_r , which is determined by material properties and serves as the characteristic length of the natural time coordinate t , describes a relatively long-term behavior compared with a single period of loading. To characterize the fast varying features of response fields induced by the locally periodic loading as shown in Figure 1, we assume that there exists a small positive scaling parameter ζ so that a fast time coordinate τ can be identified and defined as

$$\tau = t/\zeta \tag{1}$$

We further assume that the response fields are locally periodic in the time domain with respect to τ , or at least in the statistical sense. The period of external loading denoted by τ_0 serves as characteristic length of the fast time coordinate. Thus, the scaling parameter ζ can be defined as

$$\zeta = \tau_0/t_r, \quad \zeta \ll 1 \quad (2)$$

With the definition of the fast varying variable τ as well as the τ -periodicity assumption, all the response fields denoted by ϕ can be defined by using the conventional nomenclature:

$$\phi^\zeta(\mathbf{x}, t) = \phi(\mathbf{x}, t, \tau) \quad (3)$$

where \mathbf{x} denotes the position vector in space. The time differentiations in this case can be expressed using the chain rule:

$$\dot{\phi}^\zeta = \phi_{,t} + \zeta^{-1} \phi_{,\tau} \quad (4)$$

where the comma followed by a subscript variable denotes a partial derivative and superscribed dot denotes the time derivative.

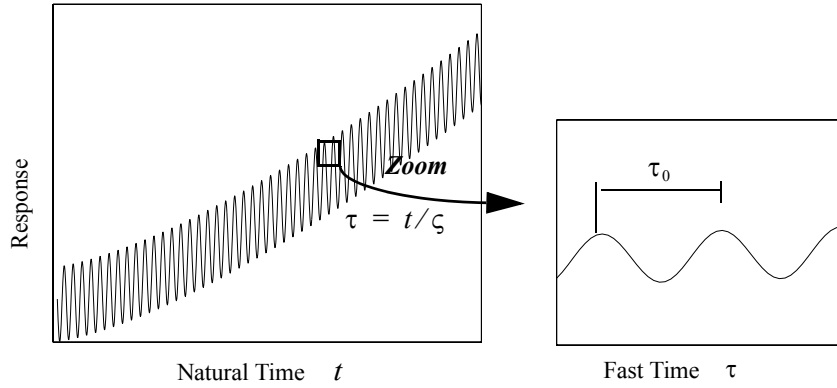


Figure 1. Natural and fast time coordinates

2.2 Temporal homogenization of the Maxwell viscoelastic solids under cyclic loading

The initial-boundary value problems for the Maxwell viscoelastic model is summarized below:

$$\text{Equilibrium equation: } \sigma_{ij,j}^\zeta + \bar{b}_i(\mathbf{x}, t, \tau) = 0 \quad \text{on } \Omega \times (0, T) \times (0, \tau_0) \quad (5)$$

$$\text{Constitutive equation: } \dot{e}_{ij}^\zeta = C_{ijkl} \dot{\sigma}_{kl}^\zeta + S_{ijkl} \sigma_{kl}^\zeta \quad \text{on } \Omega \times (0, T) \times (0, \tau_0) \quad (6)$$

$$\text{Kinematic equation: } e_{ij}^\zeta = (u_{i,j}^\zeta + u_{j,i}^\zeta)/2 \quad \text{on } \Omega \times (0, T) \times (0, \tau_0) \quad (7)$$

$$\text{Initial conditions: } u_i^\zeta(\mathbf{x}, t = \tau = 0) = \tilde{u}_i(\mathbf{x}) \quad \text{on } \Omega \quad (8)$$

$$\text{Boundary conditions: } u_i^\zeta = \bar{u}_i(\mathbf{x}, t, \tau) \quad \text{on } \Gamma_u \times (0, T) \times (0, \tau_0) \quad (9)$$

$$\sigma_{ij}^\zeta n_j = \bar{f}_i(\mathbf{x}, t, \tau) \quad \text{on } \Gamma_f \times (0, T) \times (0, \tau_0) \quad (10)$$

where \bar{b}_i is a body force; σ_{ij}^ζ and e_{ij}^ζ are the components of stress and strain tensors, respectively; C_{ijkl} represents the components of elastic compliance tensor and S_{ijkl} denotes the components of the inverse of viscosity tensor; both C_{ijkl} and S_{ijkl} are assumed to be symmetric and positive definite; u_i^ζ represents the components of displacement vector; T is the observation time in the natural time coordinates; τ_0 is the load period in the fast (scaled) time coordinates as shown in Figure 1; Ω denotes the spatial domain while Γ_u and Γ_f are the corresponding boundary portions where displacements \bar{u}_i and tractions \hat{f}_i are prescribed, respectively; n_i denotes the normal vector component on the boundary; \tilde{u}_i is the initial displacement. Summation convention for repeated subscripts is adopted.

To solve the initial-boundary value problem (5)-(10), we start by approximating the displacement field in terms of the double temporal scales asymptotic expansion

$$u_i^\zeta = \sum_{m=0,1,\dots} \zeta^m u_i^m(\mathbf{x}, t, \tau) \quad (11)$$

where u_i^m ($m = 0, 1, \dots$) are τ -periodic functions and m denotes the order of the terms in the expansion. Note that the first term in the asymptotic expansion (11) is a function of both, t and τ , to reflect the fact that the smooth and oscillatory parts of the displacement field could be of the same order of magnitude. According to (7) and the chain rule in (4), the corresponding expansions of strains and the strain rates can be expressed as

$$e_{ij}^\zeta = \sum_{m=0,1,\dots} \zeta^m e_{ij}^m(\mathbf{x}, t, \tau); \quad e_{ij}^m = (u_{j,i}^m + u_{i,j}^m)/2 \quad (12)$$

and

$$\dot{e}_{ij}^\zeta = \sum_{m=0,1,\dots} \zeta^{m-1} \dot{e}_{ij}^{m-1}(\mathbf{x}, t, \tau); \quad \dot{e}_{ij}^{-1} = e_{ij,\tau}^0 \text{ and } \dot{e}_{ij}^m = e_{ij,t}^m + e_{ij,\tau}^{m+1} \quad (13)$$

Consequently, the expansion of stresses is obtained by substituting expansions in (12) and (13) into the constitutive equation (6), which gives

$$\sigma_{ij}^\zeta = \sum_{m=0,1,\dots} \zeta^m \sigma_{ij}^m(\mathbf{x}, t, \tau) \quad (14)$$

where the stress components in the asymptotic expansion are determined from various order constitutive equations:

$$O(\zeta^{-1}): \quad e_{ij,\tau}^0 = C_{ijkl} \sigma_{kl,\tau}^0 \quad \text{on } \Omega \times (0, T) \times (0, \tau_0) \quad (15)$$

$$O(\zeta^m): \quad e_{ij,t}^m + e_{ij,\tau}^{m+1} = C_{ijkl}(\sigma_{kl,t}^m + \sigma_{kl,\tau}^{m+1}) + S_{ijkl}\sigma_{kl}^m \quad \text{on } \Omega \times (0, T) \times (0, \tau_0) \quad (16)$$

Having defined the expansions of response fields, the asymptotic expansion of the equilibrium equation can be obtained by substituting (14) into (5) which gives

$$O(\zeta^0): \quad \sigma_{ij,j}^0 + \bar{b}_i(\mathbf{x}, t, \tau) = 0 \quad \text{on } \Omega \times (0, T) \times (0, \tau_0) \quad (17)$$

$$O(\zeta^{m+1}): \quad \sigma_{ij,j}^{m+1} = 0 \quad \text{on } \Omega \times (0, T) \times (0, \tau_0) \quad (18)$$

where $m = 0, 1, \dots$. From (8)-(10), along with the asymptotic expansion (11) and (14) for displacements and stresses, the initial and boundary conditions (ICs and BCs) for the $O(\zeta^0)$ order initial-boundary problems (15)(17) are given by

$$\begin{aligned} O(\zeta^0) \text{ ICs: } \quad u_i^0(\mathbf{x}, t = \tau = 0) &= \tilde{u}_i(\mathbf{x}) \quad \text{on } \Omega \\ O(\zeta^0) \text{ BCs: } \quad u_i^0 &= \bar{u}_i(\mathbf{x}, t, \tau) \quad \text{on } \Gamma_u \times (0, T) \times (0, \tau_0) \\ \sigma_{ij}^0 n_j &= \bar{f}_i(\mathbf{x}, t, \tau) \quad \text{on } \Gamma_f \times (0, T) \times (0, \tau_0) \end{aligned} \quad (19)$$

For the high order problems defined in (16)(18), both initial and boundary conditions are trivial.

To solve (15)-(18) along with the appropriate initial and boundary conditions for various order of response fields, we introduce the temporal averaging operator $\langle \bullet \rangle$, defined as

$$\langle \bullet \rangle = \frac{1}{\tau_0} \int_0^{\tau_0} \bullet \, d\tau \quad (20)$$

as well as the following decompositions:

$$\begin{aligned} \Phi_{ij}^m(\mathbf{x}, t, \tau) &= \sigma_{ij}^m - \langle \sigma_{ij}^m \rangle \\ \Psi_{ij}^m(\mathbf{x}, t, \tau) &= e_{ij}^m - \langle e_{ij}^m \rangle \\ \chi_i^m(\mathbf{x}, t, \tau) &= u_i^m - \langle u_i^m \rangle \end{aligned} \quad (21)$$

where Φ_{ij}^m , Ψ_{ij}^m and χ_i^m represent the oscillatory portion of the stress, strain and displacement fields, respectively. From (12), we have

$$\Psi_{ij}^m = (\chi_{j,i}^m + \chi_{i,j}^m)/2; \quad m = 0, 1, \dots \quad (22)$$

For the smooth portion of the $O(1)$ order homogenized solution, the constitutive relation and the field equation can be obtained by applying temporal averaging operator (20) to (16) and (17) in the case of $m = 1$, which yields

$$\langle e_{ij}^0 \rangle_{,t} = C_{ijkl} \langle \sigma_{kl}^0 \rangle_{,t} + S_{ijkl} \langle \sigma_{kl}^0 \rangle \quad \text{on } \Omega \times (0, T) \quad (23)$$

$$\langle \sigma_{ij}^0 \rangle_{,j} + \langle \bar{b}_i(\mathbf{x}, t, \tau) \rangle = 0 \quad \text{on } \Omega \times (0, T) \quad (24)$$

where τ -periodicity of e_{kl}^1 and σ_{kl}^1 has been exploited. The corresponding initial and boundary conditions for the $O(\zeta^0)$ global initial-boundary value problem are given by averaging (18) over a single load cycle, which yields

$$\begin{aligned} \text{ICs: } \langle u_i^0 \rangle(\mathbf{x}, t = 0) &= \tilde{u}_i(\mathbf{x}) && \text{on } \Omega \\ \text{BCs: } \langle u_i^0 \rangle &= \langle \bar{u}_i(\mathbf{x}, t, \tau) \rangle && \text{on } \Gamma_u \times (0, T) \\ \langle \sigma_{ij}^0 \rangle n_j &= \langle \bar{f}_i(\mathbf{x}, t, \tau) \rangle && \text{on } \Gamma_f \times (0, T) \end{aligned} \quad (25)$$

Solutions of $\langle u_i^0 \rangle(\mathbf{x}, t)$, $\langle e_{ij}^0 \rangle(\mathbf{x}, t)$ and $\langle \sigma_{ij}^0 \rangle(\mathbf{x}, t)$ for the $O(\zeta^0)$ order initial-boundary value problem represent the non-oscillatory long-term behavior of the response fields, which is independent of the fast time variable τ .

For the oscillatory portion of the $O(\zeta^0)$ order homogenized solution, equations (15) and (21) lead to the following constitutive relation:

$$\Psi_{ij,\tau}^0 = C_{ijkl} \Phi_{kl,\tau}^0 \quad \text{on } \Omega \times (0, \tau_0) \quad (26)$$

The corresponding equilibrium equation is obtained by subtracting (24) from (17) and exploiting the definition in (21), which gives

$$\Phi_{ij,j}^0 + \bar{b}_i - \langle \bar{b}_i \rangle = 0 \quad \text{on } \Omega \times (0, \tau_0) \quad (27)$$

The initial and boundary conditions corresponding to equations (26) and (27) are given as:

$$\begin{aligned} \text{ICs: } \langle \chi_i^0 \rangle &= 0 && \text{on } \Omega \\ \text{BCs: } \chi_i^0 &= \bar{u}_i - \langle \bar{u}_i \rangle && \text{on } \Gamma_u \times (0, \tau_0) \end{aligned} \quad (28)$$

$$\Phi_{ij}^0 n_j = \bar{f}_i - \langle \bar{f}_i \rangle \quad \text{on } \Gamma_f \times (0, \tau_0)$$

It is worth noting that the initial-boundary value problem described by (22) and (26)-(28) is defined on $\Omega \times (0, \tau_0)$, i.e, it has to be solved for one load cycle only. This is because the response fields are assumed to be periodic functions of τ and the constitutive equation (26) need to be integrated with respect to τ only.

In summary, the $O(1)$ order initial-boundary problem (15)-(17) defined on $\Omega \times (0, T) \times (0, \tau_0)$ has been decomposed into two initial-boundary problems: one for the smooth long term behavior defined on $\Omega \times (0, T)$ which is independent of the fast time variable τ , and the second one on $\Omega \times (0, \tau_0)$, for a single load period evolving around the smooth solution.

A similar two-step scheme is used for solving high order initial-boundary value problems. The high order initial-boundary value problems can be obtained from (16) and (18)-(21), which yields:

For the global $O(\zeta^{m+1})$ initial-boundary value problem ($m = 0, 1, \dots$):

$$\begin{aligned} \text{Equilibrium equation: } \langle \sigma_{ij}^{m+1} \rangle_{,j} &= 0 & \text{on } \Omega \times (0, T) \\ \text{Constitutive equation: } \langle e_{ij}^{m+1} \rangle_{,t} &= C_{ijkl} \langle \sigma_{kl}^{m+1} \rangle_{,t} + S_{ijkl} \langle \sigma_{kl}^{m+1} \rangle & \text{on } \Omega \times (0, T) \end{aligned} \quad (29)$$

Trivial initial and boundary conditions.

For the local $O(\zeta^{m+1})$ initial-boundary value problem ($m = 0, 1, \dots$):

$$\begin{aligned} \text{Equilibrium equation: } \Phi_{ij,j}^{m+1} &= 0 & \text{on } \Omega \times (0, \tau_0) \\ \text{Constitutive equation: } \Psi_{ij,\tau}^{m+1} &= C_{ijkl} \Phi_{kl,\tau}^{m+1} + (C_{ijkl} \Phi_{kl,t}^m + S_{ijkl} \Phi_{kl}^m - \Psi_{ij,t}^m) & \text{on } \Omega \times (0, \tau_0) \\ \text{Initial conditions: } \langle \chi_i^{m+1} \rangle &= 0 & \text{on } \Omega \quad (30) \\ \text{Boundary conditions: } \chi_i^{m+1} &= 0 & \text{on } \Gamma_u \times (0, \tau_0) \\ \Phi_{ij}^{m+1} n_j &= 0 & \text{on } \Gamma_f \times (0, \tau_0) \end{aligned}$$

The solution of (29) is trivial, i.e., the only contribution from the high order equations comes from the local initial-boundary value problem. Hence, $\Phi_{ij}^{m+1} = \sigma_{ij}^{m+1}$, $\Psi_{ij}^{m+1} = e_{ij}^{m+1}$ and $\chi_i^{m+1} = u_i^{m+1}$ where $m = 0, 1, \dots$

2.3 Temporal homogenization of the viscoplastic solid subjected to locally periodic loading

In this section, we develop a temporal homogenization scheme for the power-law viscoplastic solid [10]. The initial-boundary value problem in this case takes a similar form to that described in Section 2.2 (see equation (5), (7)-(9)), except for the constitutive equation which is given as

$$\dot{\sigma}_{ij}^{\zeta} = L_{ijkl}(\dot{e}_{kl}^{\zeta} - \dot{\mu}_{kl}^{\zeta}) \quad (31)$$

where e_{kl}^{ζ} denotes the elastic strain components defined in (12) and μ_{kl}^{ζ} is postulated as a viscoplastic strain which follows the power-law form flow rule:

$$\begin{aligned} \dot{\mu}_{kl}^{\zeta} &= \lambda^{\zeta} N_{kl}^{\zeta} \\ \lambda^{\zeta} &= a \left\{ \frac{\sqrt{3}}{\sqrt{2}} \|\xi_{ij}^{\zeta}\| / Y^{\zeta} \right\}^{1/c} \\ N_{kl}^{\zeta} &= \xi_{kl}^{\zeta} / \|\xi_{kl}^{\zeta}\| \end{aligned} \quad (32)$$

where a and c are material constants; ξ_{kl}^{ζ} is termed as the effective stress defined as

$$\xi_{kl}^{\zeta} = P_{kl ij}(\sigma_{ij}^{\zeta} - \beta_{ij}^{\zeta}); \quad \|\xi_{kl}^{\zeta}\| = \sqrt{\xi_{kl}^{\zeta} \xi_{kl}^{\zeta}} \quad (33)$$

where $P_{kl ij} = I_{kl ij} - \delta_{ij} \delta_{kl} / 3$ is a projector, which transfers $(\sigma_{ij}^{\zeta} - \beta_{ij}^{\zeta})$ to the deviatoric space; δ_{ij} is the Kronecker delta and $I_{kl ij} = \frac{1}{2}(\delta_{ik} \delta_{jl} - \delta_{il} \delta_{jk})$; β_{ij}^{ζ} is often referred to as the back stress while Y^{ζ} in (32) is the drag stress. For simplicity, we assume that β_{ij}^{ζ} and Y^{ζ} follow linear hardening rules [13]:

$$\begin{aligned} \dot{\beta}_{ij}^{\zeta} &= \frac{2}{3} H \dot{\mu}_{ij}^{\zeta} \\ Y^{\zeta} &= \hat{Y} - \alpha^{\zeta}; \quad \dot{\alpha}^{\zeta} = \sqrt{\frac{2}{3}} \hat{H} \lambda^{\zeta} \end{aligned} \quad (34)$$

where H , \hat{H} and \hat{Y} are material constants assumed to be independent of the viscoplastic flow.

To obtain the asymptotic expansion of the stress fields, we introduce the following expansion for the viscoplastic strain μ_{ij}^{ζ} along with the assumption (11) for the displacement u_i^{ζ} :

$$\mu_{ij}^{\zeta} = \sum_{m=0,1,\dots} \zeta^m \mu_{ij}^m(\mathbf{x}, t, \tau) \quad (35)$$

where all the components in the expansion are assumed to be locally periodic functions of the fast time variable τ . From the definition in (35), together with the constitutive equation (31), the flow rule (32) and the hardening rule (34), it can be shown that the asymptotic expansion of σ_{ij}^{ζ} , β_{ij}^{ζ} and α^{ζ} are given as:

$$\begin{aligned} \sigma_{ij}^{\zeta} &= \sum_{m=0,1,\dots} \zeta^m \sigma_{ij}^m(\mathbf{x}, t, \tau) \\ \beta_{ij}^{\zeta} &= \sum_{m=0,1,\dots} \zeta^m \beta_{ij}^m(\mathbf{x}, t, \tau) \\ \alpha^{\zeta} &= \sum_{m=0,1,\dots} \zeta^m \alpha^m(\mathbf{x}, t, \tau) \end{aligned} \quad (36)$$

The expansion of the norm of the effective stress $\|\xi_{kl}^{\zeta}\|$ defined in (33) is given by

$$\|\xi_{kl}^{\zeta}\| = \|\xi_{kl}^0\| (1 + \zeta R)^{1/2} \quad (37)$$

where

$$\xi_{kl}^0 = P_{kl ij}(\sigma_{ij}^0 - \beta_{ij}^0); \quad R = 2 \xi_{kl}^0 \xi_{kl}^1 / \|\xi_{kl}^0\| + O(\zeta) \quad (38)$$

Since $|\zeta R| \ll 1$ equation (37) can be further expanded as

$$\|\xi_{kl}^{\zeta}\| = \|\xi_{kl}^0\| \left(1 + \frac{1}{2} \zeta R - \frac{1}{8} \zeta^2 R^2 + O(\zeta^3) \right) = \|\xi_{kl}^0\| + O(\zeta) \quad (39)$$

Similarly, the expansion of the viscoplastic flow parameter λ^{ζ} and the flow direction vector N_{kl}^{ζ} defined in (32) can be expressed as

$$\lambda^{\zeta} = \lambda^0(\mathbf{x}, t, \tau) + O(\zeta) = a \left\{ \frac{\sqrt{3}}{2} \|\xi_{ij}^0\| / (\hat{Y} - \alpha^0) \right\}^{1/c} + O(\zeta) \quad (40)$$

$$N_{kl}^{\zeta} = N_{kl}^0(\mathbf{x}, t, \tau) + O(\zeta) = \xi_{kl}^0 / \|\xi_{kl}^0\| + O(\zeta) \quad (41)$$

and thus the two leading order expansions of the flow rule (32) take the following form:

$$O(\zeta^{-1}): \quad \mu_{kl,\tau}^0 = 0 \quad (42)$$

$$O(\zeta^0): \quad \mu_{kl,t}^0 + \mu_{kl,\tau}^1 = \lambda^0 N_{kl}^0 \quad (43)$$

where (42) indicates that the leading order viscoplastic strain is independent of τ , i.e. $\mu_{kl}^0 \equiv \mu_{kl}^0(\mathbf{x}, t)$. Furthermore, as a result of (40) and (42), the $O(\zeta^0)$ back stress β_{ij}^0 and drag stress Y^0 defined in (34) are also independent of τ so that the $O(\zeta^0)$ expansion of (34) is given by

$$\begin{aligned} \beta_{ij,t}^0 + \beta_{ij,\tau}^1 &= \frac{2}{3} H \lambda^0 N_{ij}^0 \\ Y^0 = \hat{Y} - \alpha^0; \quad \alpha_{ij,t}^0 + \alpha_{ij,\tau}^1 &= \sqrt{\frac{2}{3}} \hat{H} \lambda^0 \end{aligned} \quad (44)$$

where $\beta_{ij}^0 \equiv \beta_{ij}^0(\mathbf{x}, t)$ and $\alpha_{ij}^0 \equiv \alpha_{ij}^0(\mathbf{x}, t)$.

Having defined the expansions in (12), (36), and (40)-(44), we can obtain the asymptotic expansion of the constitutive equation (31):

$$O(\zeta^{-1}): \quad \sigma_{ij,\tau}^0 = L_{ijkl} e_{kl,\tau}^0 \quad \text{on } \Omega \times (0, T) \times (0, \tau_0) \quad (45)$$

$$O(\zeta^m): \quad \sigma_{ij,t}^m + \sigma_{ij,\tau}^{m+1} = L_{ijkl} \{ (e_{kl}^m - \mu_{kl}^m)_{,t} + (e_{kl}^{m+1} - \mu_{kl}^{m+1})_{,\tau} \} \quad \text{on } \Omega \times (0, T) \times (0, \tau_0) \quad (46)$$

where $m = 0, 1, \dots$ and the definition of the elastic strain components e_{kl}^m is given in (13).

We note that the asymptotic expansions of the equilibrium equation and initial-boundary conditions in this case are the same as those for the Maxwell viscoelastic model derived in Section 2.2 (see equations (17)-(19)). To solve the various order initial-boundary problems, we follow the decompositions defined in (21) so that various order initial-boundary value problems can be again solved in two steps, first for the whole loading history and the second for one period of load cycle. Following the procedure described in Section 2.2, the initial-boundary value problems for the responses fields of various order can be summarized as follows:

For the local $O(\zeta^0)$ initial-boundary value problem (using (45)):

$$\text{Equilibrium equation:} \quad \Phi_{ij,j}^0 + b_i^\zeta - \langle b_i^\zeta \rangle = 0 \quad \text{on } \Omega \times (0, \tau_0)$$

$$\text{Constitutive equation:} \quad \Phi_{ij,\tau}^0 = L_{ijkl} \Psi_{kl,\tau}^0 \quad \text{on } \Omega \times (0, \tau_0)$$

$$\text{Initial condition: } \langle \chi_i^0 \rangle = 0 \quad \text{on } \Omega \times (0, \tau_0) \quad (47)$$

$$\text{Boundary conditions: } \chi_i^0 = \bar{u}_i - \langle \bar{u}_i \rangle \quad \text{on } \Gamma_u \times (0, \tau_0)$$

$$\Phi_{ij}^1 n_j = \tilde{f}_i - \langle \tilde{f}_i \rangle \quad \text{on } \Gamma_f \times (0, \tau_0)$$

For the global $O(\zeta^0)$ initial-boundary value problem (using (46)):

$$\text{Equilibrium equation: } \langle \sigma_{ij}^0 \rangle_{,j} + \langle b_i^5 \rangle = 0 \quad \text{on } \Omega \times (0, T)$$

$$\text{Constitutive equation: } \langle \sigma_{ij}^0 \rangle_{,t} = L_{ijkl} \{ \langle e_{kl}^0 \rangle_{,t} - \langle \mu_{kl}^0 \rangle_{,t} \} \quad \text{on } \Omega \times (0, T)$$

$$\text{Initial condition: } \langle u_i^0 \rangle(\mathbf{x}, t = 0) = \tilde{u}_i(\mathbf{x}) \quad \text{on } \Omega \times (0, T) \quad (48)$$

$$\text{Boundary conditions: } \langle u_i^0 \rangle = \langle \bar{u}_i(\mathbf{x}, t, \tau) \rangle \quad \text{on } \Gamma_u \times (0, T)$$

$$\langle \sigma_{ij}^0 \rangle n_j = \langle \tilde{f}_i(\mathbf{x}, t, \tau) \rangle \quad \text{on } \Gamma_f \times (0, T)$$

where the plastic strain rate $\langle \mu_{kl}^0 \rangle_{,t}$ is obtained by averaging (43) over one period of load cycle, which yields

$$\langle \mu_{kl}^0 \rangle_{,t} = \langle \lambda^0 N_{kl}^0 \rangle \quad (49)$$

with λ^0 and N_{kl}^0 defined in (40) and (41). The corresponding back stress and drag stress are governed by the temporal average of (44):

$$\beta_{ij,t}^0 = \frac{2}{3} H \langle \lambda^0 N_{ij}^0 \rangle \quad (50)$$

$$Y^0 = \hat{Y} - \alpha^0; \quad \alpha_{ij,t}^0 = \sqrt{\frac{2}{3}} \hat{H} \langle \lambda^0 \rangle$$

where the τ -periodicity has been applied. Note that the flow rule is a function of the total stress $\langle \sigma_{kl}^0 \rangle + \Phi_{kl}^0$, which provides a one-way coupling between the global and local initial-boundary value problems. In the one-way coupled scheme, Φ_{kl}^0 is computed first by solving the local problem (47) at each time increment of the global problem (48), except when the loading in (47) is independent of the natural time variable t in which case the local contribution can be precomputed ahead of global analysis. Subsequently, the global initial-boundary value is solved for the next time increment.

Note that the constitutive equation for the oscillatory portion of $O(\zeta^0)$ homogenized solutions in (47) is linear while the constitutive equations for the high order oscillations remain nonlinear according to (46). Also, the smooth portion of the high order homogenized solution is generally non-trivial in contrast to the solution for the Maxwell viscoelastic model.

3.0 One-dimensional verification examples

In this section, the analytical and numerical solutions for the one-dimensional homogenized problems are compared with the reference solutions in order to verify the present temporal homogenization scheme.

3.1 One-dimensional solution of the Maxwell viscoelastic model

Consider a one-dimensional bar clamped at one end ($x = 0$) and subjected to loading at the other end ($x = d$) as shown in Figure 1. A sinusoidal displacement with a period of $\tau_0 = 2\pi/\omega$ superimposed on the constant field, $\bar{u}^\zeta = U_0(\sin \omega t + 1)$, is chosen as a prescribed displacement. According to [15], the material intrinsic time scale for the one-dimensional Maxwell viscoelastic model can be defined as

$$t_r = V/L \quad (51)$$

where V denotes the viscosity, L is elastic stiffness, and t_r is the creep time. We assume that the period of loading is much smaller than the material intrinsic time scale so that $\zeta = \tau_0/t_r \ll 1$. The prescribed displacement expressed in terms of the fast time coordinate is given as

$$\bar{u}^\zeta(x = 0, t, \tau) = U_0(\sin \omega t + 1) = U_0\left(\sin \frac{2\pi}{t_r} \tau + 1\right) \quad (52)$$

where U_0 is the amplitude of the prescribed displacement and ω is the radial frequency of the load.

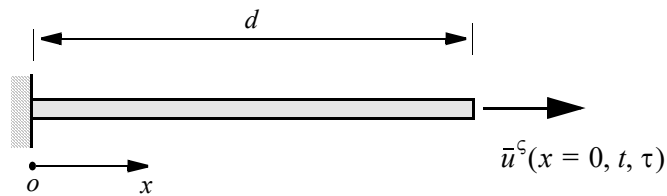


Figure 2. One-dimensional bar and the oscillatory loading

Following (5)-(9), the reference solution for the strain field in one-dimensional viscoelastic problem can be obtained by solving

$$\frac{\dot{\sigma}^\zeta}{L} + \frac{\sigma^\zeta}{V} = \frac{U_0 \omega}{d} \cos \omega t; \quad \sigma^\zeta(t=0) = \frac{LU_0}{d} \quad (53)$$

where σ^ζ denotes the axial stress. The solution of (53) is given as

$$\sigma^\zeta = \frac{LU_0}{d} \left\{ \left(1 - \frac{\omega t_r}{1 + \omega^2 t_r^2} \right) \exp\left(-\frac{t}{t_r}\right) + \frac{\omega^2 t_r^2}{1 + \omega^2 t_r^2} \left(\sin \omega t + \frac{1}{\omega t_r} \cos \omega t \right) \right\} \quad (54)$$

where t_r follows from (51). Since the scaling parameter ζ is $\zeta = 2\pi/\omega t_r \ll 1$, equation (54) can be approximated as:

$$\sigma^\zeta = \frac{LU_0}{d} \left(\exp\left(-\frac{t}{t_r}\right) + \sin \omega t \right) + O(\zeta) \quad (55)$$

The homogenized solutions for the one-dimensional viscoelastic problem can be obtained by reducing the equations in Section 2.2 to the one-dimensional case. Noting that $\tau = t/\zeta$ according to (1), the leading order initial-boundary problem can be summarized as follows:

The $O(1)$ global initial-boundary value problem:

$$\begin{aligned} \langle \sigma^0 \rangle_{,x} &= 0 && \text{on } (0, T) \\ \frac{\langle \sigma^0 \rangle_{,t}}{L} + \frac{\langle \sigma^0 \rangle}{V} &= \langle e^0 \rangle_{,t}; && \langle e^0 \rangle(x, t) = \langle u^0 \rangle_{,x}(x, t) \\ \langle u^0 \rangle(t=0) &= 0; && \langle u^0 \rangle(x=0) = 0; \quad \langle u^0 \rangle(x=d) = U_0 \end{aligned} \quad (56)$$

The $O(1)$ local initial-boundary value problem:

$$\begin{aligned} \Phi_{,x}^0 &= 0 && \text{on } (0, \tau_0) \\ \Phi_{,\tau}^0 &= L\Psi_{,\tau}^0; && \Psi^0(x, t, \tau) = \chi_{,x}^0(x, t, \tau) \\ \chi^0(\tau=0) &\text{ is defined in such a way that } \langle \Phi^0 \rangle = 0 \\ \chi^0(x=0) &= 0; && \chi^0(x=d) = U_0 \sin \omega t = U_0 \sin \frac{2\pi}{t_r} \tau \end{aligned} \quad (57)$$

The $O(1)$ analytical solution of the initial-boundary value problem (56)-(58) is given by:

$$\sigma^\zeta = \frac{LU_0}{d} \left\{ \exp\left(-\frac{t}{t_r}\right) + \sin\omega t \right\} + O(\zeta) \quad (58)$$

which coincides with the corresponding reference solution (55) provided that $\zeta \ll 1$.

3.2 One-dimensional solution for the power-law viscoplastic model

The loading is assumed to be the same as in (52) defined in Section 3.1. Following Section 2.3, the source initial-boundary value problem can be stated as:

$$\begin{aligned} \sigma_{,x}^\zeta &= 0 && \text{on } (0, T) \\ \dot{\sigma}^\zeta &= L(\dot{e}^\zeta - \dot{\mu}^\zeta); && e^\zeta = u_{,x}^\zeta; \quad \dot{\mu}^\zeta = a(|\xi^\zeta|/Y^\zeta)^{1/c} \text{sgn}(\xi^\zeta) \\ \xi^\zeta &= \sigma^\zeta - \beta^\zeta; && Y^\zeta = \hat{Y} - \alpha^\zeta \\ \dot{\beta}^\zeta &= H\dot{\mu}^\zeta; && \dot{\alpha}^\zeta = \hat{H}\dot{\mu}^\zeta \text{sgn}(\xi^\zeta) \\ u^\zeta(t=0) &= U_0; && u^\zeta(x=0) = 0; \quad u^\zeta(x=d) = U_0(\sin\omega t + 1) \end{aligned} \quad (59)$$

The closed form solution of (59) exists only when $H = \hat{H} = 0$ and $c = 1$. For this case, the reference solution of the stress field can be obtained by solving the linear initial value problem

$$\begin{aligned} \dot{\sigma}^\zeta + \frac{aL}{\hat{Y}}\sigma^\zeta &= \frac{LU_0\omega}{d} \cos\omega t \\ \sigma^\zeta(t=0) &= LU_0/d \end{aligned} \quad (60)$$

It can be seen that equation (60) is similar to (53) and thus the solution can be expressed in the form of equation (55) where the material intrinsic time scale is defined as $t_r = \hat{Y}/aL$ and the scaling parameter is given as $\zeta = 2\pi/\omega t_r \ll 1$. In the second part of this section, we will consider a general case of (59) with nonzero hardening parameter and $c \neq 1$.

Following Section 2.3, the leading order one-dimensional homogenized solution can be obtained by solving the following two initial-boundary value problems.

The $O(1)$ local initial-boundary value problem:

$$\begin{aligned}
\Phi^0_{,x} &= 0 && \text{on } (0, \tau_0) \\
\Phi^0_{,\tau} &= L\Psi^0_{,\tau}; && \Psi^0 = \chi^0_{,x} \\
\chi^0(\tau = 0) &\text{ is defined in such a way that } \langle \Phi^0 \rangle = 0 \\
\chi^0(x = 0) &= 0; && \chi^0(x = d) = U_0 \sin \omega t = U_0 \sin \frac{2\pi}{t_r} \tau
\end{aligned} \tag{61}$$

The solution of (61), which is a linear problem, can be easily obtained as

$$\Phi^0 = \frac{LU_0}{d} \left(\sin \frac{2\pi}{t_r} \tau \right) = \frac{LU_0}{d} \sin \omega t \tag{62}$$

The $O(1)$ global initial-boundary value problem:

$$\begin{aligned}
\langle \sigma^0 \rangle_{,x} &= 0 && \text{on } (0, T) \\
\langle \sigma^0 \rangle_{,t} &= L \{ \langle e^0 \rangle_{,t} - \langle \mu^0 \rangle_{,t} \}; && \langle e^0 \rangle = \langle u^0 \rangle_{,x}; \quad \langle \mu^0 \rangle_{,t} = a \langle (|\xi^0|/Y^0)^{1/c} \text{sgn}(\xi^0) \rangle \\
\xi^0 &= \langle \sigma^0 \rangle + \Phi^0 - \beta^0; && Y^0 = \hat{Y} - \alpha^0 \\
\beta^0_{,t} &= H \langle \mu^0_{,t} \rangle; && \alpha^0_{,t} = \hat{H} \langle \mu^0_{,t} \text{sgn}(\xi^0) \rangle \\
u^0(t = 0) &= U_0; && u^0(x = 0) = 0; \quad u^0(x = d) = U_0
\end{aligned} \tag{63}$$

Similarly to (59), the analytical solution of (61) can be found for $H = \hat{H} = 0$ and $c = 1$. In this case, $O(1)$ order smooth stress field is given by

$$\langle \sigma^0 \rangle = \frac{LU_0}{d} \exp\left(-\frac{t}{t_r}\right) \tag{64}$$

Thus the total $O(1)$ stress field obtained by adding the contributions from equations (62) and (64) coincides with the reference solutions given in (54) and (55).

To this end we consider a more general viscoplastic material model where all the nonlinearities are taken into account. The geometry of the one-dimensional bar is shown in Figure 2. The loading is assumed to be in the form of prescribed displacement $\bar{u}^s = U_0(0.1 \sin \omega t + 1)$. The amplitude of the loading is taken as $U_0/d = 2 \times 10^{-3}$ and the radial frequency $\omega = 20\pi \text{ s}^{-1}$ so that $\tau_0 = 0.1 \text{ s}$. We select material properties as $L = 50 \text{ GPa}$, $\hat{Y} = 100 \text{ MPa}$, $H = 4 \text{ GPa}$, $\hat{H} = 0$, $a = 5 \times 10^{-4} \text{ s}^{-1}$, and $c = 0.7$. Numerical solution for source problem (59) is obtained by using a very fine time increment

for the entire loading history. The comparison between the $O(1)$ smooth homogenization solution and the reference solution is given in Figure 3. It can be seen that $\langle \sigma^0 \rangle$ captures well the non-oscillatory long-term behavior. In Figure 4, we show the $O(1)$ oscillatory stress field for two load cycles, one at the early stage of the loading at $[0.9, 1.0s]$ and second, at the end of the loading $[9.9s, 10s]$. Good agreement with the reference solution can be observed.

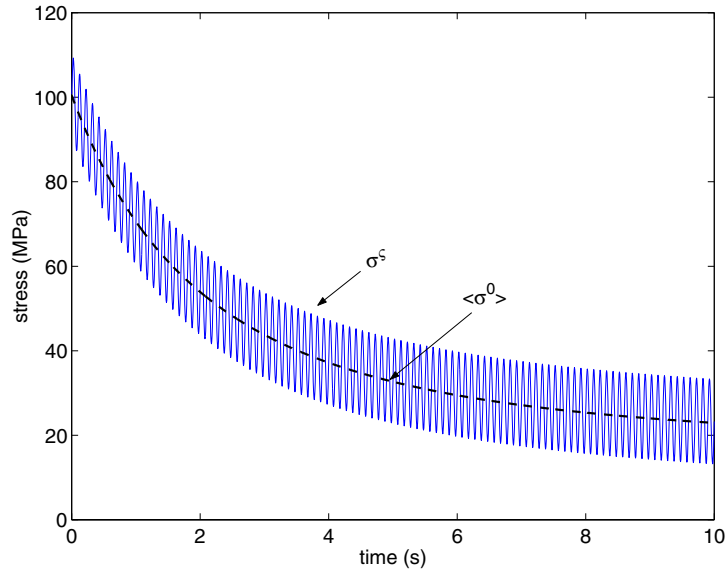


Figure 3. $O(1)$ global solution in comparison with reference solutions for the one-dimensional viscoplastic model

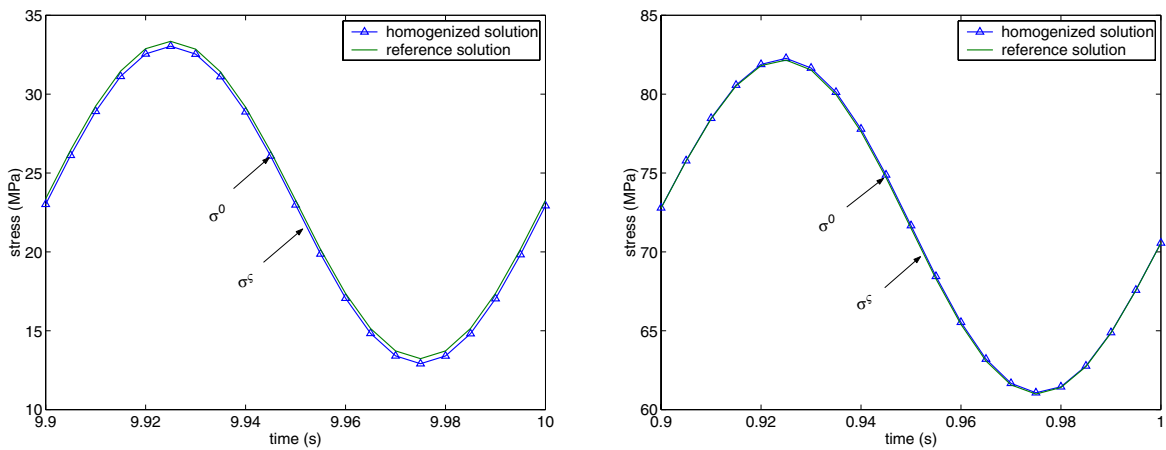


Figure 4. $O(1)$ homogenized solution in comparison with reference solutions for the one-dimensional viscoplastic model

4.0 Numerical Examples in 3D

4.1 Four-point bending of viscoelastic beam

We first consider a four-point bending problem with a configuration shown in Figure 5. The beam is made of isotropic viscoelastic material of Maxwell type. The material properties are selected as $E = 50\text{GPa}$, $\nu = 0.3$ and $V = 200\text{GPa}\cdot\text{hr}$, where E is Young's modulus, ν denotes Poisson's ratio, and V is viscosity. The load applied to the cross heads is in the form of prescribed displacement

$$\bar{u}_2^\zeta = U_0 \{0.1 \sin \omega t + 1 - \exp(-t/2t_r)\} \quad (65)$$

where U_0 is the amplitude and ω is the radial frequency. The load period is given by $\tau_0 = 2\pi/\omega$. According to (2), ζ defines the ratio between the loading period τ_0 and the intrinsic time scale t_r for the Maxwell viscoelastic model, where t_r can be estimated by [15]:

$$t_r = O\{\|V_{ijkl}\|/\|L_{ijkl}\|\} \quad (66)$$

where $\|\bullet\|$ represents the norm of \bullet . Thus, the intrinsic time scale in this example is estimated as $t_r = 1.6$ hr and the load frequency is chosen as $\omega = 10\pi \text{ hr}^{-1}$, i.e. 5 cycles per hour, so that $\zeta = 2\pi/\omega t_r = 0.125$. The load amplitude U_0 is chosen as $U_0 = -0.4\text{mm}$.

Numerical results for the maximum tensile strain component, e_{33}^ζ , at the bottom surface in the mid span, as well as its $O(1)$ temporal average, $\langle e_{33}^0 \rangle$, are shown in Figure 6. As in the one-dimensional case, $\langle e_{33}^0 \rangle$ provides a good approximation of the non-oscillatory portion of the long-term solution. Similar observations can be made for the stress field shown in Figure 7. In Figure 8 and Figure 9, we show the total strains and stresses recovered by postprocessing in the two time windows. It can be seen that the leading order homogenized solution agrees well with the reference solution.

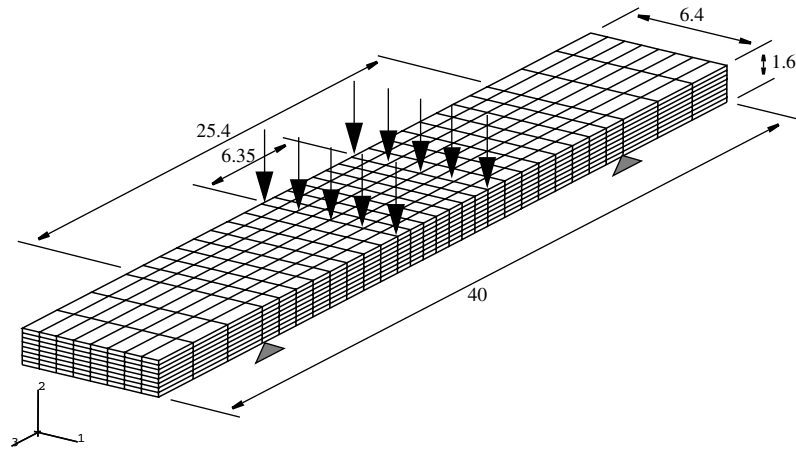


Figure 5. Configuration and FE mesh for the four-point bending problem

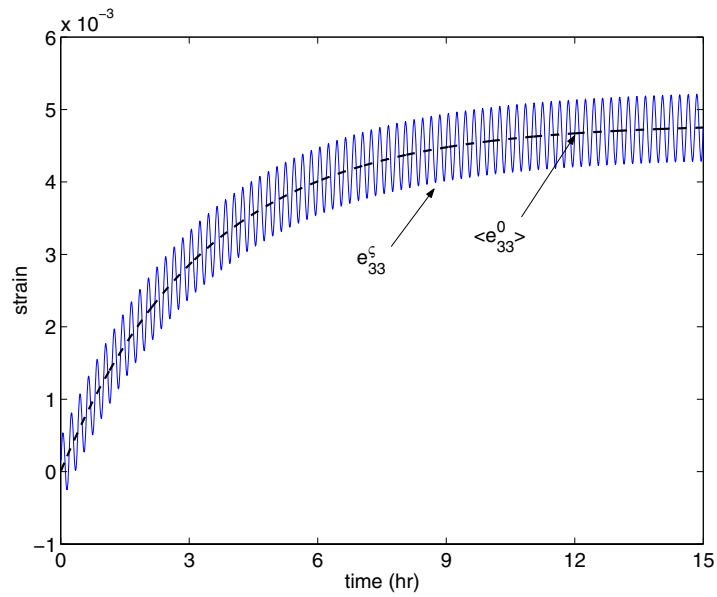


Figure 6. Reference solution versus $O(1)$ global solution for the maximum strain

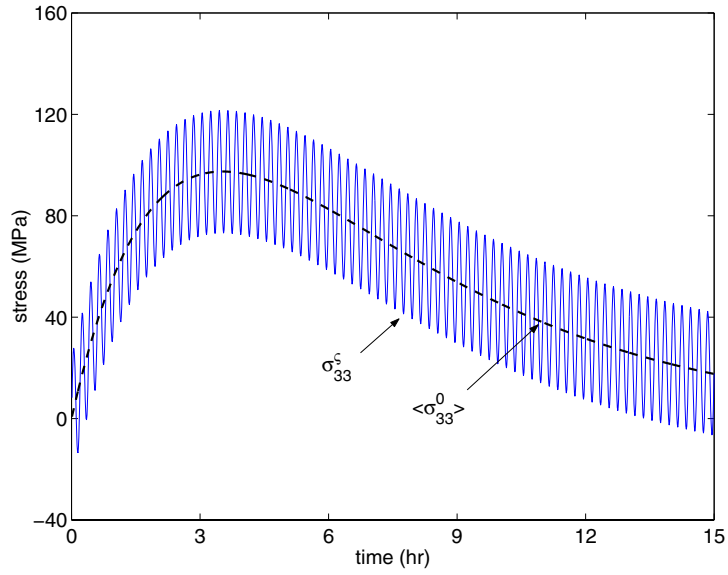


Figure 7. Reference solution versus $O(1)$ global solution for the maximum stress

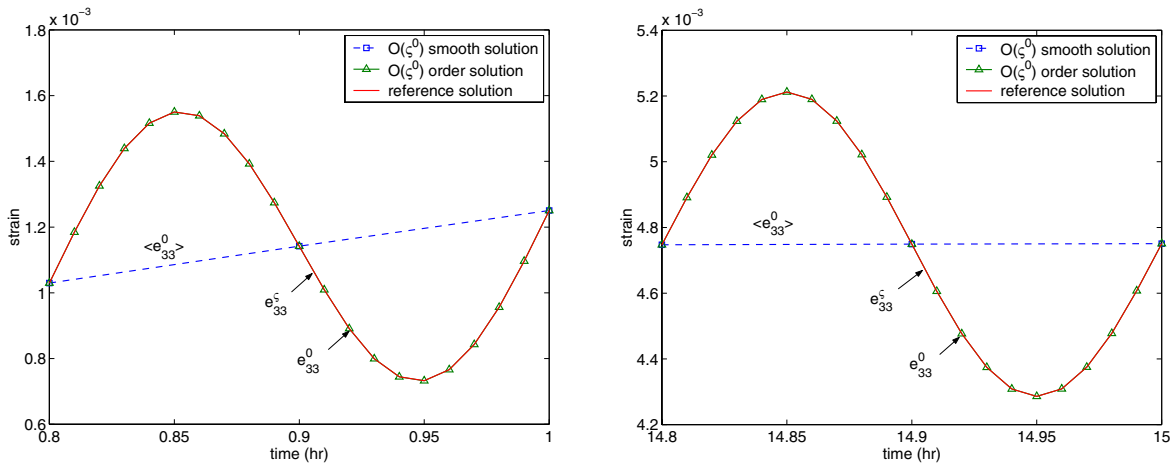


Figure 8. Reference solutions versus $O(1)$ homogenized solution for the maximum strain

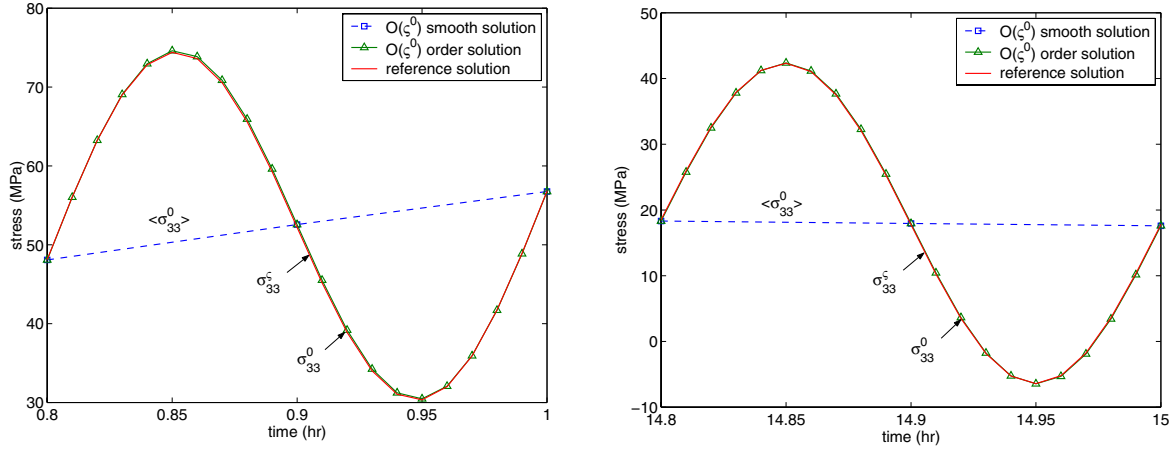


Figure 9. Reference solutions versus $O(1)$ homogenized solution for the maximum stress

4.2 The nozzle flap problem for the power-law viscoplastic model

The finite element mesh of the half of the nozzle flap (due to symmetry) is shown in Figure 10. The flap is subjected to an aerodynamic force which is simulated by a superposition of the uniform constant pressure and a sinusoidal loading with an amplitude equal to 10% of the value of the constant pressure and the load period of one cycle per minute, i.e., $\omega = 120\pi \text{ hr}^{-1}$. The loading is applied on the flat surface. We assume that the pin eyes are rigid and not allowed to rotate so that all degrees of freedom on the pin eye surfaces are fixed. The nozzle flap is made of type 316 stainless steel which exhibits a viscoplastic behavior in room temperature. Material constants in the power-law viscoplastic model are obtained by fitting the creep test data provided in [3]. Material properties are summarized below:

Type 316 stainless steel: $L = 185\text{GPa}$, $\nu = 0.3$, $\bar{Y} = 95\text{MPa}$, $H = 320\text{GPa}$, $\hat{H} = 0$,
 $a = 2 \times 10^{-8} \text{ hr}^{-1}$, and $c = 0.1$

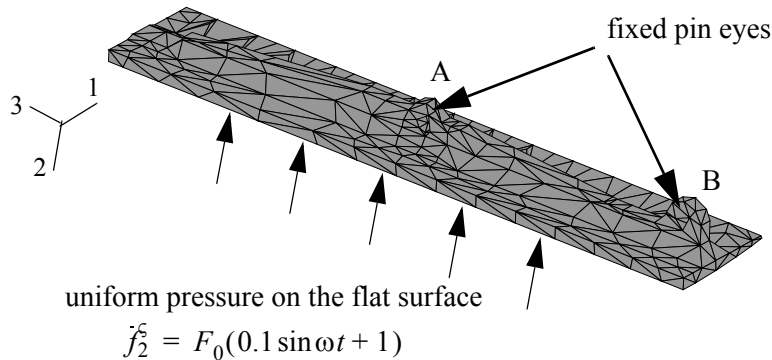


Figure 10. FE mesh for the nozzle flap

Numerical results reveal that the maximum stress and strain components (in direction 2) occur on the inner surface of the pin eye A. Figure 11 and Figure 12 depict the history of maximum stresses and strains as obtained with the reference solution (using very small time increment step) and the $O(1)$ temporal homogenization (with postprocessing) solutions. In Figure 13, the $O(1)$ response fields at the end of loading, including displacement, stress and strain fields, are compared with the corresponding reference solutions. In all the cases considered the $O(1)$ response fields agree well with the reference solution.

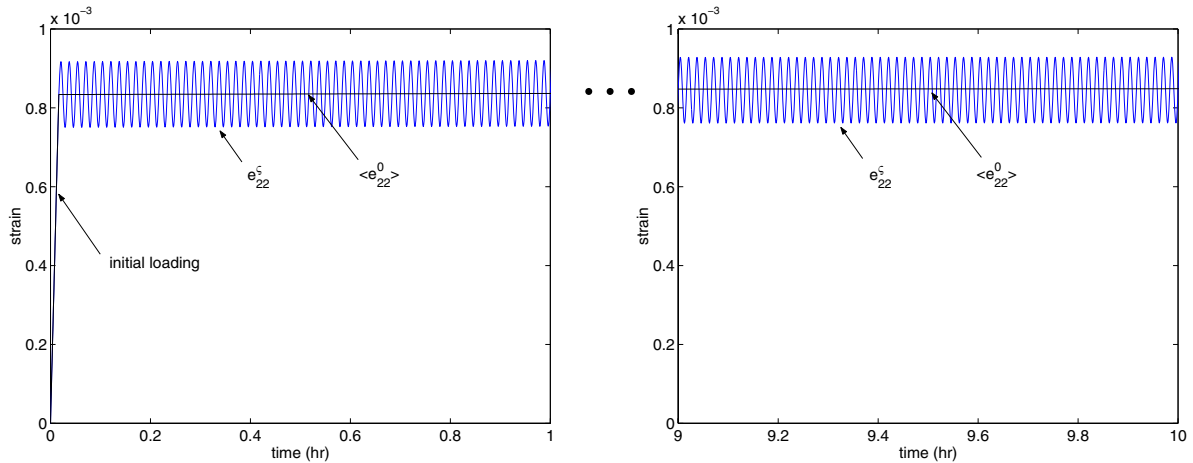


Figure 11. Reference solution e_{22}^c versus $O(1)$ global homogenized solution $\langle e_{22}^0 \rangle$ at the pin eye A

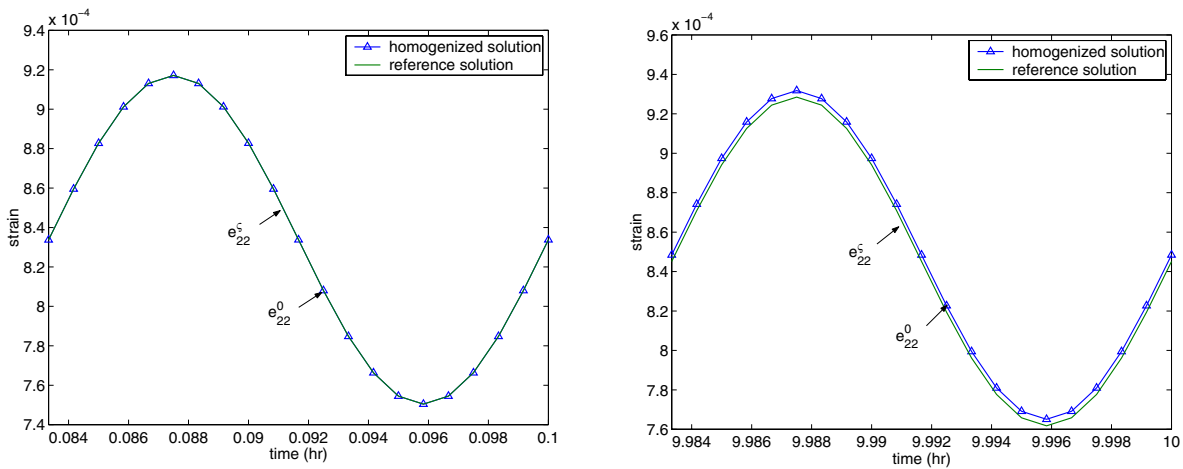


Figure 12. Reference solution e_{22}^c versus $O(1)$ homogenized solution e_{22}^0 at the pin eye A

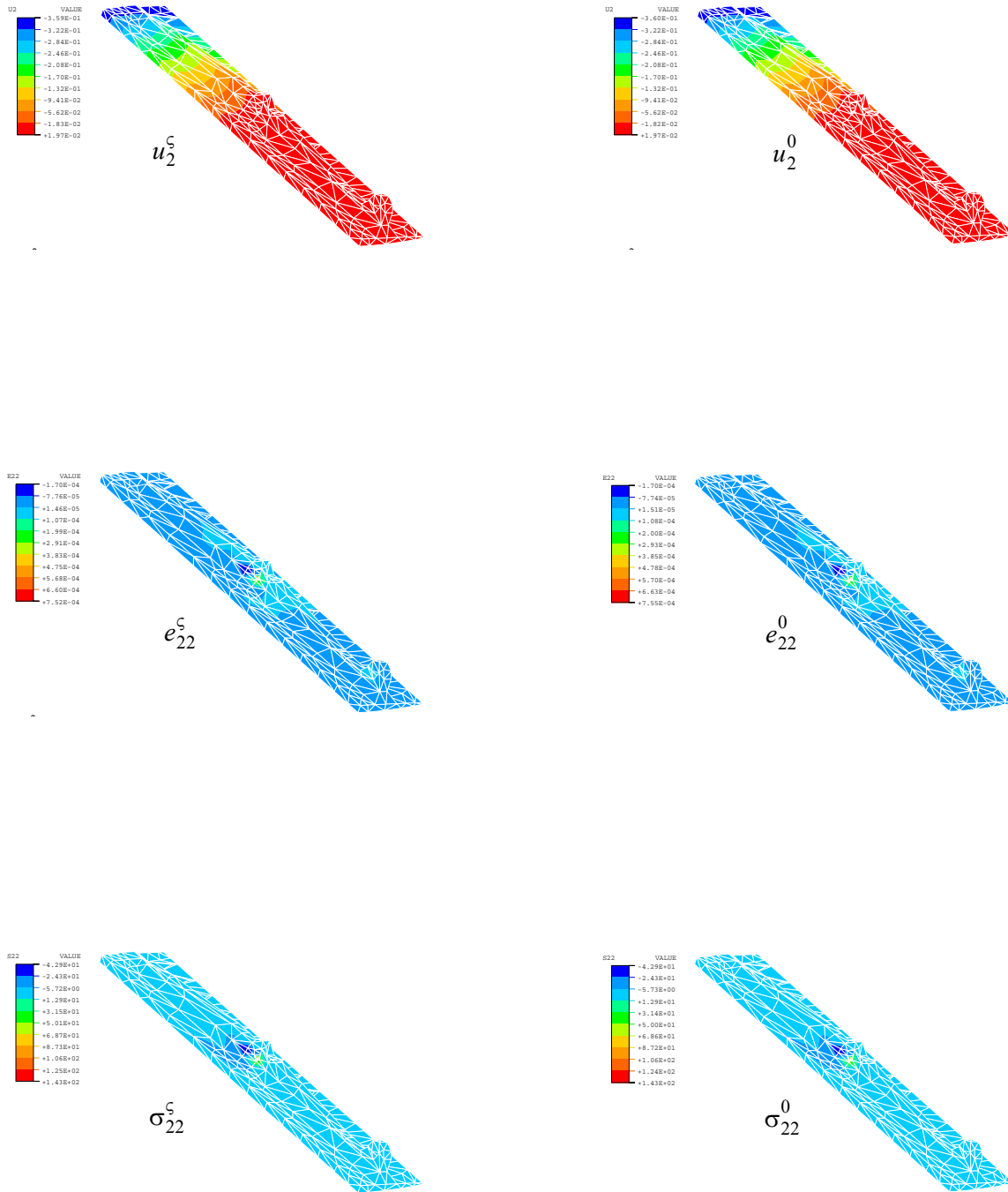


Figure 13. Reference solution versus $O(1)$ homogenized solution for the nozzle flap problem

5.0 Concluding Remark

The asymptotic temporal homogenization formulation for viscoelastic and viscoplastic models has been developed to resolve multiple temporal scales. The scaling parameter is defined as the ratio between the material intrinsic time and the frequency of load period. It is shown that a long-term response can be obtained by solving the temporally averaged leading order homogenized initial-boundary value problem along with the smooth portion of the external loading. The leading order oscillatory behavior, which represents the deviation from the smooth solutions, is obtained by solving a linear initial-boundary value problems for one period of load cycle. The global and local initial-boundary value problems for the linear Maxwell viscoelastic model are decoupled, whereas for the viscoplastic model, local analysis has to be performed at each global time increment. In both cases, large time increments can be used for the global problem with smooth loading, while the integration of the local initial-boundary value problem requires a significantly smaller time step, but only locally in a single load period. The present temporal homogenization approach has been found to be in good agreement with the reference solution as long as the scaling parameter remains small.

In our future work the present temporal homogenization scheme will be extended to fatigue of homogeneous solids. If successful, the methodology will be then generalized to fatigue analysis of heterogeneous solids, which are characterized by multiple temporal and spatial scales.

6.0 Acknowledgement

This work was supported by the Sandia National Laboratories under Contract DE-AL04-94AL8500 and the Office of Naval Research through grant number N00014-97-1-0687.

References

- 1 Bensoussan, A., Lions, J.L. Papanicolaou, G., 1978. *Asymptotic Analysis for Periodic Structures*, North-Holland, Amsterdam.
- 2 Boutin, C., Wong, H., 1998. Study of thermosensitive heterogeneous media via space-time homogenisation. *European Journal of Mechanics: A/Solids*, 17, 939-968.
- 3 Chaboche, J.L. and Rousselier, G., 1983. On the plastic and viscoplastic constitutive equation-Part II: Application of internal variable concept to the 316 stainless steel, *Journal of Pressure Vessel Technology*, 105, 159-164.
- 4 Chen, W., Fish, J., 2001. A dispersive model for Wave propagation in periodic composites based on homogenization with multiple spatial and temporal scales. *Journal of Applied Mechanics*, 68(2), 153-161.
- 5 Fish, J. and Chen, W., 2001. Uniformly Valid Multiple Spatial-Temporal Scale Modeling for Wave Propagation in Heterogeneous Media. *Mechanics of Composite Materials and Structures*, 8, 81-99.
- 6 Fish, J. and Chen, W., and Nagai, G., 2001. Nonlocal dispersive model for wave propagation in heterogeneous media: One-Dimensional Case. *International Journal for Numerical Methods in*

Engineering, in print.

- 7 Fish, J. and Chen, W., and Nagai, G., 2001. Nonlocal dispersive model for wave propagation in heterogeneous media: Multi-Dimensional Case. *International Journal for Numerical Methods in Engineering*, in print.
- 8 Francfort, G.A., 1983. Homogenization and linear thermoelasticity. *SIAM Journal of Mathematical Analysis*, 14, 696-708
- 9 Kevorkian, J., Bosley, D.L., 1998. Multiple-scale homogenization for weakly nonlinear conservation laws with rapid spatial fluctuations. *Studies in Applied Mathematics*, 101, 127-183.
- 10 Odqvist, F.K.G., 1974. *Mathematical Theory of Creep and Creep Rupture*, Clarendon Press, Oxford.
- 11 Pierce, D, Shih, C.F., and Needleman, A., 1984. A tangent modulus method for rate dependent solids, *Computers and Structures*, 18, 875-887.
- 12 Sanchez-Palencia, E., 1980. *Non-Homogeneous Media and Vibration Theory*, Springer-Verlag, Berlin.
- 13 Simo, J.C. and Hughes, T.J.R., 1998. *Computational Inelasticity*, Springer-Verlag New York, Inc., New York.
- 14 Suquet, P.M., 1987. Elements of homogenization for inelastic solid mechanics. In: *Homogenization Techniques for Composite Media*, eds. Sanchez-Palencia, E. and Zaoui, A., Springer-Verlag, Berlin, pp193-278.
- 15 Yu, Q. and Fish J., 2001. Multiscale asymptotic homogenization for multiphysics problems with multiple spatial and temporal scales: A couple thermo-mechanical example problem, *International Journal of Solids and Structures*, submitted in 2001